

The Modulating Effect of Mechanical Changes in Lipid Bilayers Caused by ApoE-Containing Lipoproteins on $\text{A}\beta$ Induced Membrane Disruption

Justin Legleiter,^{*†} John D. Fryer,[‡] David M. Holtzman,^{‡,§,||} and Tomasz Kowalewski^{*‡}

[†]The C. Eugene Bennett Department of Chemistry, WVnano Initiative, the Center for Neurosciences, West Virginia University, 217 Clark Hall, P.O. Box 6045, Morgantown, West Virginia 26506, United States

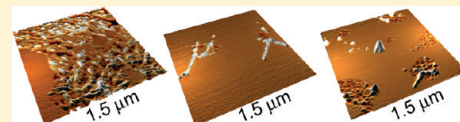
[‡]Department of Neurology, Washington University School of Medicine, St. Louis, Missouri 63110, United States

[§]Hope Center for Neurological Disorders, Washington University School of Medicine, 660 South Euclid Avenue, Box 8111, St. Louis, Missouri 63110, United States

^{||}Department of Developmental Biology, Washington University School of Medicine, St. Louis, Missouri 63110, United States

^{*}Department of Chemistry, Carnegie Mellon University, 4400 Fifth Avenue, Pittsburgh, Pennsylvania 15213, United States

ABSTRACT: A major feature of Alzheimer's disease (AD), a late-onset neurodegenerative disorder, is the ordered aggregation of the β -amyloid peptide ($\text{A}\beta$) into fibrils that comprise extracellular neuritic plaques found in the disease brain. One of many potential pathways for $\text{A}\beta$ toxicity may be modulation of lipid membrane function. Here, we show by *in situ* atomic force microscopy (AFM) that astrocyte secreted lipoprotein particles (ASLPs) containing different isoforms of apolipoprotein E (apoE), of which the apoE4 allele is a major risk factor for the development of AD, can protect total brain lipid extract bilayers from $\text{A}\beta_{1-40}$ induced disruption. The apoE4 allele was less effective in protecting lipid bilayers from disruption compared with apoE3. Size analysis of apoE-containing ASLPs and mechanical studies of bilayer properties revealed that apoE-containing ASLPs modulate the mechanical properties of bilayers by acquiring some bilayer components (most likely cholesterol and/or oxidatively damaged lipids). Measurement of bilayer mechanical properties was accomplished with scanning probe acceleration microscopy (SPAM). These measurements demonstrated that apoE4 was also less effective in modulating mechanical properties of bilayers in comparison with apoE3. This ability of apoE to alter the mechanical properties of lipid membranes may represent a potential mechanism for the suppression of $\text{A}\beta_{1-40}$ induced bilayer disruption.



KEYWORDS: Apolipoprotein E, amyloid- β , lipid bilayer, cholesterol, atomic force microscopy, Alzheimer's disease

The ordered aggregation of the β -amyloid peptide ($\text{A}\beta$) as extracellular neuritic plaques in the brain is a major hallmark associated with Alzheimer's disease (AD).^{1,2} $\text{A}\beta$ is a primarily $\sim 39\text{--}42$ amino acid long cleavage product of the amyloid precursor protein (APP), a transmembrane protein. The insoluble aggregated form of $\text{A}\beta$, which deposits in the extracellular space in the brain and on the walls of cerebral blood vessels,³ exhibits an enhanced β -sheet content as opposed to the partially α -helical soluble form found in body fluids.^{4,5} It has been hypothesized that a potential pathway for $\text{A}\beta$ toxicity may be due to its ability to modulate lipid membrane function. This hypothesis is based on the observation that $\text{A}\beta$ bears a portion of the APP transmembrane domain. Thus, elucidating the interaction between $\text{A}\beta$ and membrane lipids could be critical in understanding potential pathways of $\text{A}\beta$ toxicity, especially given the results of studies that demonstrate that changes in membrane composition occur in AD along with the association with plaques, tangles, and neuritic dystrophy.^{6–10} Possible toxic effects of $\text{A}\beta$ interactions with membranes include disruption of the bilayer structure, changes in bilayer curvature, and/or the creation of membrane pores or channels.^{11–22}

Atomic force microscopy (AFM) studies of the interaction of $\text{A}\beta_{1-40}$ with bilayers formed from total brain lipid extract

(TBLE) revealed that, over time, $\text{A}\beta_{1-40}$ aggregation resulted in large-scale bilayer disruption associated with large fiberlike structures.²³ Further studies of TBLE bilayers explored the effect of cholesterol on disruption and $\text{A}\beta$ aggregation.²⁴ The susceptibility of TBLE bilayers to $\text{A}\beta_{1-40}$ induced disruption was strongly dependent on the cholesterol content of the bilayer. Neither the bilayers in which cholesterol content was increased (by the addition of up to 30% exogenous cholesterol) nor cholesterol-depleted bilayers (achieved by the use of methyl- β -cyclodextrin) were disrupted by $\text{A}\beta_{1-40}$ over a period of 9–15 h. Aggregation of $\text{A}\beta_{1-40}$ also appeared to be facilitated by the presence of TBLE bilayers, since no $\text{A}\beta_{1-40}$ aggregation has been observed in solutions of $\text{A}\beta_{1-40}$ over the same incubation time.^{23,24} These results suggest that $\text{A}\beta$ -induced membrane disruption could be used as a model system to study the effect of relevant biomacromolecules and complexes on this process.

A disease-related exogenous factor that could potentially modulate $\text{A}\beta$ interactions with supported lipid bilayers is lipoproteins containing apoE. ApoE is a 34 kDa apolipoprotein that

Received: May 20, 2011

Accepted: July 14, 2011

Published: July 14, 2011

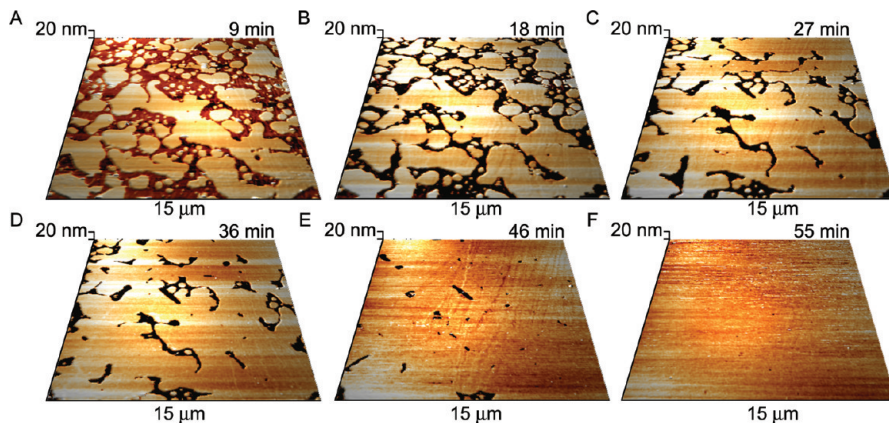


Figure 1. Time-lapse sequence of AFM images of the same surface area demonstrating the evolution of a TBLE bilayer on mica in the process of vesicle fusion. Almost immediately after contacting mica, vesicles formed round bilayer patches (A), which then gradually fused into an increasingly continuous bilayer (B–E), eventually reaching a predominately defect-free stage (F), providing a model surface for studying $\text{A}\beta$ aggregation.

has a carboxyl terminal domain that interacts with lipids and an amino terminal domain that interacts with several cell surface receptors.^{25,26} There are three main isoforms of human apoE: apoE2, apoE3, and apoE4 which are products of the $\epsilon 2$, $\epsilon 3$, and $\epsilon 4$ alleles present on a single gene locus on chromosome 19.²⁷ ApoE is present in the central nervous system (CNS) and appears to function in the extracellular transport of lipids during development and repair.^{28,29} In the CNS, apoE is primarily produced and secreted by astrocytes³⁰ and microglia^{31,32} and is present in HDL-like particles in the cerebrospinal fluid.^{29,33} The $\epsilon 4$ allele of apoE has been shown to be a major risk factor in early onset AD and has been associated with increased amyloid load in the AD brain and mouse models of AD,^{34–38} suggesting that different variants of apoE may affect the rate of formation of amyloid plaques. The exact relationship between AD, $\text{A}\beta$, and apoE remains unclear, but numerous possibilities for this relationship have been postulated. ApoE can promote the aggregation and transition of $\text{A}\beta$ into fibrils,^{39,40} affect the deposition of $\text{A}\beta$ in mouse models of AD,⁴¹ participate in $\text{A}\beta$ metabolism in the CNS,⁴² and has been shown to have antioxidant activity.⁴³

Herein, we explore the effect of apoE3- and apoE4-containing astrocyte-secreted lipoprotein particles (ASLPs) on $\text{A}\beta$ -aggregation and their ability to disrupt TBLE bilayers. This is accomplished through direct observations of bilayer disruption with the aid of in situ AFM. This study makes use of direct observation of bilayer disruption by $\text{A}\beta_{1–40}$ via in situ AFM, followed by quantitative analysis of AFM images and the indirect measurement of bilayer mechanical properties. Analysis of bilayer mechanical properties was accomplished with scanning probe acceleration microscopy (SPAM).⁴⁴

RESULTS AND DISCUSSION

$\text{A}\beta_{1–40}$ Induced Membrane Disruption. Bilayers used in this study were produced through the fusion of TBLE vesicles on mica (Figure 1). Bilayers formed by TBLE provide an excellent model surface for in situ AFM studies, as they are composed of a physiologically relevant ratio of membrane components, that is, acidic and neutral phospholipids, gangliosides, cholesterol, sphingolipids, and isoprenoids. The time needed to form a predominately defect-free bilayer is also significantly reduced under the influence of the scanning AFM tip, as areas not imaged exhibit less vesicle fusion within 50–100 min of injection of lipid

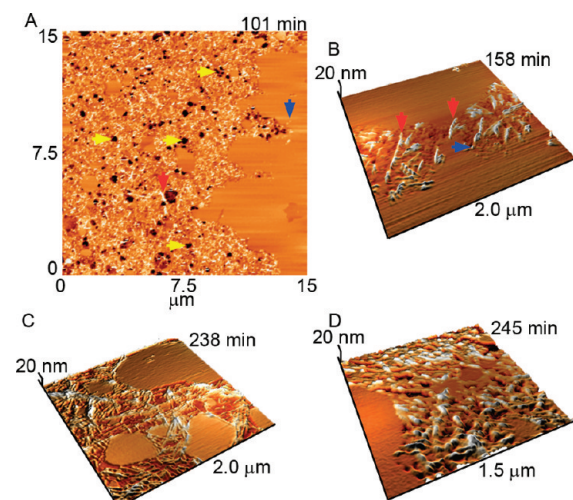


Figure 2. In situ AFM images illustrating disruption of TBLE bilayers supported on mica by fresh solutions of $\text{A}\beta_{1–40}$ (final concentration of $\text{A}\beta$ was $9.6 \mu\text{g/mL}$). In the large area scan (A), the left portion of the bilayer underwent nearly total disruption, manifested as bilayer roughening or holes, which extends all the way to the mica surface (indicated by yellow arrows). Higher magnification 3D images (B–D) reveal that disrupted bilayer regions formed around fibrillar (B, C) and oblong (D) objects, resembling $\text{A}\beta$ aggregates typically observed by AFM (see Figure 4). Bilayers were supported on mica substrates. Examples of oligomeric and fibrillar aggregates are indicated by blue and red arrows, respectively.

vesicles into the fluid cell compared with continuously imaged areas. This could be due to the force exerted when pushing vesicles to the surface and flattening them, thus facilitating their fusion. Such vesicle fusion into planar bilayers is well-known.⁴⁵

Experiments were conducted with $\text{A}\beta_{1–40}$ to verify observations of TBLE bilayer disruption by $\text{A}\beta_{1–40}$ from the literature.^{23,24} Initially, when aliquots of freshly prepared solutions of $\text{A}\beta_{1–40}$ were added to the TBLE bilayers (final concentration of $9.6 \mu\text{g/mL}$), discrete aggregates of $\text{A}\beta$ appeared on (possibly in) the bilayer. After 1–2 h, patches of increased bilayer roughness appeared that were surrounded by undisturbed lipid bilayer (Figure 2). Often these areas of increased bilayer roughness were associated with globular oligomers and elongated

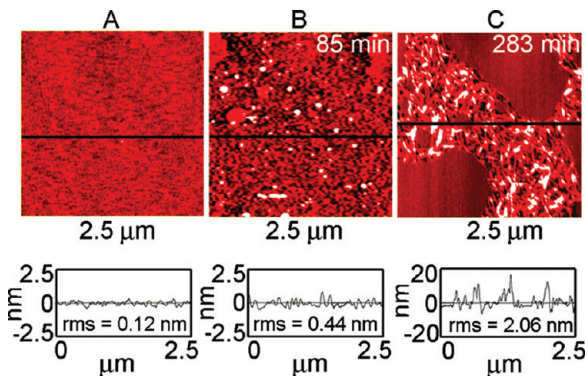


Figure 3. Quantitative assessment of $A\beta_{1-40}$ bilayer disruption by analysis of height profiles and rms roughness of images taken before (A) and after (B,C) exposure to $A\beta_{1-40}$ at a final concentration of 9.6 $\mu\text{g}/\text{mL}$. Black lines in the images correspond to the profiles shown below each image.

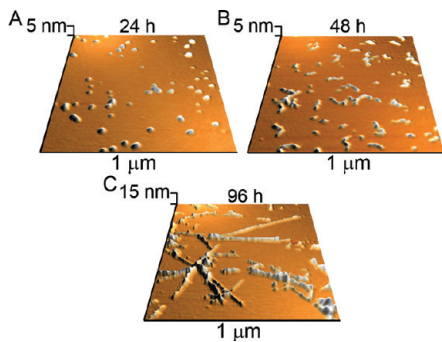


Figure 4. AFM images of typical $A\beta$ aggregates forming in “free” solution: globular species (A), protofibrils (B), and mature fibrils (C). These aggregates were deposited on mica and imaged in air. For $A\beta_{1-40}$, mature fibrils appeared after $\sim 4-6$ days of incubation at room temperature.

fibrils. The oligomers were predominately 2.5–5 nm in height with an aspect ratio smaller than 2.5 (longest distance across to shortest distance across), which indicated a predominantly round, globular structure. Fibrils were defined as having an aspect ratio larger than 2.5, which indicates an elongated structure, and the height of fibrils was typically 5–10 nm. A freshly formed bilayer had a root-mean-square (rms) surface roughness of ~ 0.12 nm measured over $6.25 \mu\text{m}^2$ (Figure 3A). After exposure to $A\beta_{1-40}$, areas appeared on the bilayer with an increased rms surface roughness of ~ 0.44 nm measured over $6.25 \mu\text{m}^2$ (Figure 3B), and as fibrils formed, the surface roughness of areas associated with fibrils reached as high as 2 nm measured over $4 \mu\text{m}^2$ to exclude areas of remaining intact bilayers seen in the image from the analysis (Figure 3C). The fraction of bilayer surface area exhibiting some amount of increased roughness was quite large ($41.6\% \pm 15.9\%$ averaged over four experiments). At longer times, holes that extended all the way through the bilayer to the mica substrate appeared. The TBLE bilayers contained on average 6.1 ± 0.9 (SD) fibrils/ μm^2 at 5 h after addition of $A\beta_{1-40}$. The observation of elongated protofibrillar and fibrillar aggregates associated with membrane disruption is striking at such short time scales (within 2–10 h at 9.6 $\mu\text{g}/\text{mL}$ as seen in Figure 2) given that similar structures appeared in the 48 $\mu\text{g}/\text{mL}$ stock solution of $A\beta_{1-40}$ stored at room temperature only after

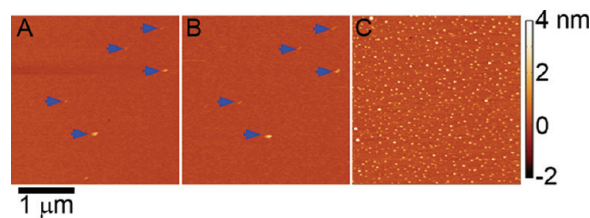


Figure 5. In situ AFM images illustrating that apoE-containing ASLPs are not incorporated into or absorbed onto the bilayer. Images of a TBLE bilayer (A) before and (b) 60 min after exposure to 30 $\mu\text{g}/\text{mL}$ of apoE3-containing ASLPs demonstrate that no substantial morphological changes to the bilayer occur. The blue arrows indicate features that were present in both images, which verify these are images of the same area. In comparison, (C) a large number of particles appear on a mica surface within 60 min upon exposure to solutions of 30 $\mu\text{g}/\text{mL}$ of apoE3-containing ASLPs.

4–6 days (Figure 4). This indicates that the presence of the TBLE lipid bilayer facilitates the aggregation of $A\beta$ into higher order structures as previously observed.^{23,24} Due to instrument heating, the temperature of solution imaged under AFM may have been slightly higher than that in stock solutions incubated at room temperature. However, the $A\beta$ in the atomic force microscope was also more dilute than the stock solution (9.6 $\mu\text{g}/\text{mL}$ compared to 48 $\mu\text{g}/\text{mL}$). Interestingly, fresh, that is, less than 1 day old, solutions of $A\beta_{1-40}$ were needed to induce bilayer disruption, implying that monomeric or small oligomeric forms of $A\beta_{1-40}$ are necessary to disrupt bilayers and suggesting that larger aggregates are unable to insert into the bilayer to cause disruption. This observation is potentially important in elucidating how different forms of $A\beta$ are toxic. To control for any influence of the AFM tip on $A\beta$ aggregation and $A\beta$ -induced bilayer disruption, only a small portion of the bilayer was continuously scanned. This allowed for areas that had not been continually scanned after the addition of $A\beta$ to be imaged at later time points for comparison. The scanning AFM tip did not have any discernible effect on $A\beta$ aggregation or $A\beta$ -induced bilayer disruption.

ApoE3- and ApoE4-Containing ASLPs Are Protective against Membrane Disruption. TBLE bilayers were exposed to ASLPs for an hour before the addition of $A\beta_{1-40}$. After this hour, limited morphological changes of the TBLE bilayers or discrete ASLPs were observed, suggesting that ASLPs were not incorporated into or absorbed onto the bilayer (Figure 5A,B). This is in direct contrast to the numerous ASLPs that are observed at the same concentrations on mica within 1 h when imaged in solution by AFM (Figure 5C). Results of in situ AFM observations of bilayer interactions with $A\beta_{1-40}$ in the presence of ASLPs containing apoE3 and apoE4 are shown in Figure 6A–D. When TBLE bilayers were pretreated with apoE3-containing ASLPs, $A\beta_{1-40}$ bilayer disruption was inhibited (no increased surface roughness observed) to varying extents, depending on lipoprotein concentration. At a concentration of 30 $\mu\text{g}/\text{mL}$ of apoE3-containing ASLPs, no increased bilayer roughness was observed after 9 h. Aggregate formation was also inhibited (Figure 6A) with fewer fibrils (0.05 ± 0.02 (SD) fibrils/ μm^2 after ~ 5 h) appearing on the bilayer surface in comparison to bilayers exposed to $A\beta$ alone (Figure 6E). At a concentration of 10 $\mu\text{g}/\text{mL}$ of apoE3-containing ASLPs, elongated fibrillar species appeared more frequently (0.3 ± 0.2 (SD) fibrils/ μm^2 after ~ 5 h). Some of these fibrillar aggregates were associated with minimal bilayer disruption; however, the vast majority of the

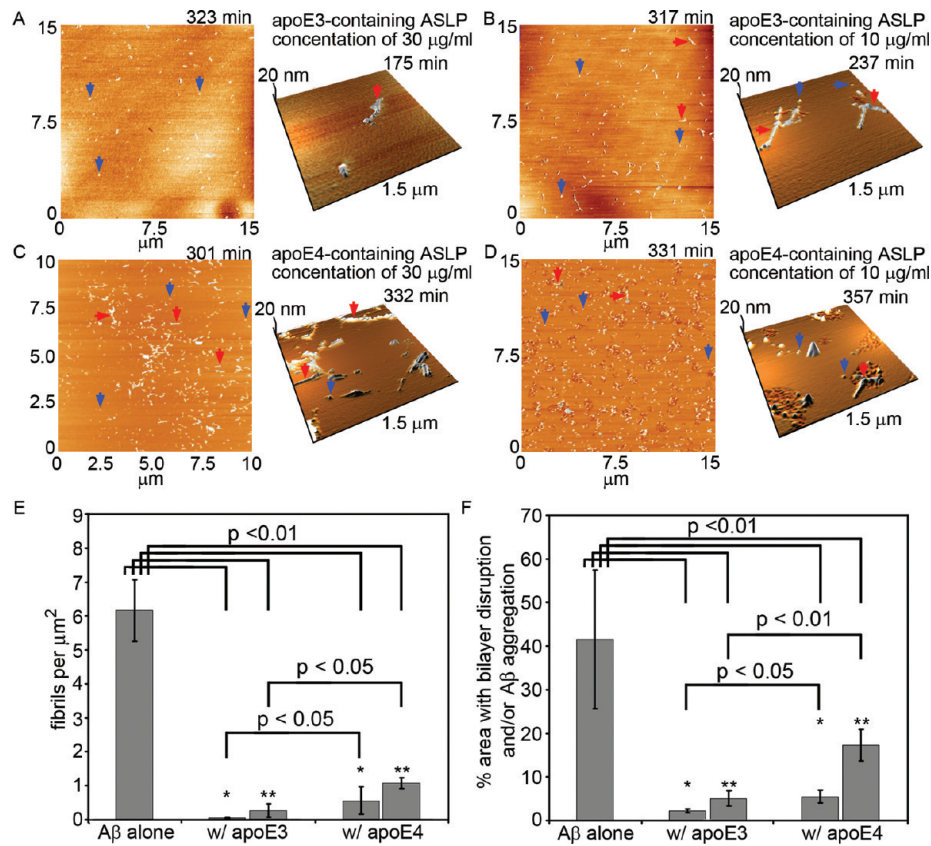


Figure 6. In situ AFM images illustrating the impact of apoE3- or apoE4-containing ASLPs on the interaction of TBLE bilayers with $\text{A}\beta_{1-40}$. In all AFM images, examples of oligomeric and fibrillar aggregates of $\text{A}\beta_{1-40}$ are indicated by blue and red arrows, respectively. AFM images of TBLE bilayers pretreated with apoE3-containing ASLPs at concentrations of (A) 30 $\mu\text{g}/\text{mL}$ and (B) 10 $\mu\text{g}/\text{mL}$ before exposure to $\text{A}\beta_{1-40}$ demonstrate that apoE3-containing ASLPs prevented bilayer disruption induced by $\text{A}\beta_{1-40}$, and only a limited number of aggregates were observed. AFM images of TBLE bilayers pretreated with apoE4-containing ASLPs at concentrations of (C) 30 $\mu\text{g}/\text{mL}$ and (D) 10 $\mu\text{g}/\text{mL}$ before exposure to $\text{A}\beta$ demonstrate that apoE4-containing ASLPs also prevented bilayer disruption and aggregate formation of $\text{A}\beta_{1-40}$, but to a lesser extent than their apoE3 counterparts. For all images in (A–D), the time stamps indicate the elapsed time after the initial exposure of the bilayer to $\text{A}\beta_{1-40}$. (E) The number of fibrils per μm^2 on TBLE bilayers was quantified in several images for each condition taken 5–6 h after the addition of $\text{A}\beta_{1-40}$. Both apoE3- and apoE4-containing ASLPs significantly reduced the number of fibrils formed by $\text{A}\beta_{1-40}$ ($p < 0.01$). A *t* test was used to compare the number of fibrils per μm^2 in bilayers pretreated with 30 $\mu\text{g}/\text{mL}$ of apoE3 to apoE4 and 10 $\mu\text{g}/\text{mL}$ of apoE3 to apoE4. Both comparisons were significantly different to the $p < 0.05$ confidence level. (F) The percent area of TBLE bilayers containing increased roughness and/or $\text{A}\beta_{1-40}$ aggregates 5 h after the addition of $\text{A}\beta_{1-40}$ was determined. Both apoE3- and apoE4-containing ASLPs significantly reduced bilayer disruption and aggregation by $\text{A}\beta_{1-40}$ ($p < 0.01$). A *t* test was used to compare disruption/aggregation in the 30 $\mu\text{g}/\text{mL}$ samples of apoE3 to apoE4 and the 10 $\mu\text{g}/\text{mL}$ samples of apoE3 to apoE4. ApoE3 treated bilayers had significantly less disruption/aggregation than apoE4 treated bilayers with $p < 0.05$ and 0.01, respectively, for the 30 $\mu\text{g}/\text{mL}$ and 10 $\mu\text{g}/\text{mL}$ treatments. For (E,F), * Indicates an ASLP concentration of 30 $\mu\text{g}/\text{mL}$, and ** indicates an ASLP concentration of 10 $\mu\text{g}/\text{mL}$. Error bars in (E,F) indicate the standard deviation for data acquired across several separate experiments. There were four independent experiments performed with $\text{A}\beta_{1-40}$ alone and with pretreatment with 30 $\mu\text{g}/\text{mL}$ apoE3-containing ASLPs. All other experimental conditions were performed in triplicate.

fibrils observed were not (Figure 6B). For comparison to bilayers exposed to $\text{A}\beta$ alone without pretreatment with apoE3-containing ASLPs, the total surface area of the bilayer that was disrupted (increased surface roughness) and/or contained $\text{A}\beta$ aggregates was measured. ApoE3-containing ASLPs reduced this area to $2.28\% \pm 0.41\%$ at 30 $\mu\text{g}/\text{mL}$ and $5.08\% \pm 1.69\%$ at 10 $\mu\text{g}/\text{mL}$ (Figure 6F). Both reductions were significant to $p < 0.01$.

At a concentration of 30 $\mu\text{g}/\text{mL}$ of apoE4-containing ASLPs, bilayer disruption was minimal for up to 9 h, yet fibril formation associated with the bilayer was still observed (Figure 6C). At a concentration of 10 $\mu\text{g}/\text{mL}$ of apoE4-containing ASLPs, the supported bilayers were disrupted (increased surface roughness) by the addition of $\text{A}\beta_{1-40}$ (Figure 6D), but to a lesser extent than nontreated bilayers. The disruption was manifested as small patches of increased rms surface roughness on the order of 0.4 nm. Many of these patches occurred in the immediate

vicinity of elongated fibrils; however, others appeared to be fibril-free. In contrast to experiments on bilayers exposed to $\text{A}\beta$ without pretreatment with ASLPs, no holes spanning the entire bilayer were observed. This observation indicates that the disruption process was suppressed to some extent even at this low concentration of apoE4-containing ASLPs. For comparison to experiments performed without pretreatment with apoE4-containing ASLPs before the addition of $\text{A}\beta_{1-40}$, the total surface area of the bilayer that was disrupted (increased surface roughness) and/or contained $\text{A}\beta$ aggregates was again measured. ApoE4-containing ASLPs reduced this area to $5.50\% \pm 1.46\%$ at 30 $\mu\text{g}/\text{mL}$ and $17.3\% \pm 3.6\%$ at 10 $\mu\text{g}/\text{mL}$ (Figure 6F). Both reductions were significant to $p < 0.01$.

In contrast to apoE3-containing ASLPs, treatment of TBLE bilayers with various concentrations of apoE4-containing ASLPs resulted in the appearance of more $\text{A}\beta_{1-40}$ fibrils (0.6 ± 0.4 (SD)

and 1.1 ± 0.2 (SD) fibrils/ μm^2 for treatment with 30 and 10 $\mu\text{g}/\text{mL}$ of apoE4, respectively, as seen in Figure 6E). The increases in the number of fibrils observed in the presence of apoE4 at each concentration were significant to the 0.05 confidence level by a *t* test compared to apoE3-containing ASLP treatment at the same concentration. However, apoE4-containing ASLPs were still able to significantly reduce the number of fibrils compared to controls without any ASLP pretreatment (Figure 6E). Although apoE4-containing ASLPs suppressed bilayer disruption by $\text{A}\beta$, it was less effective compared to apoE3-containing ASLPs. While there were fewer aggregates observed on the TBLE bilayers with pretreatment with both apoE3- and apoE4-containing ASLPs, the morphologies of the observed aggregates were indistinguishable from those formed on untreated bilayers. For example, oligomers (aggregates with an aspect ratio smaller than 2.5) were still predominately 2.5–5 nm in height, and fibrils (aggregates with an aspect ratio greater than 2.5) were typically 5–10 nm in height. When using a simple *t* test, the % area of bilayer containing disruption and/or $\text{A}\beta$ aggregates was significantly different between apoE3- and apoE4-containing ASLP pretreated bilayers at concentrations of both 10 and 30 $\mu\text{g}/\text{mL}$ (Figure 6F).

The direct interaction between the apoE-containing ASLPs and $\text{A}\beta$ was explored through incubation experiments using ex situ AFM, according to the protocol established in studies of inhibition of $\text{A}\beta$ fibrillogenesis by anti- $\text{A}\beta$ antibodies.⁴⁶ Whereas those studies clearly revealed various degrees of fibrillogenesis inhibition by different antibodies, apoE-containing ASLPs had no discernible effect on aggregation (data not shown). This suggests that the impact of lipoproteins on $\text{A}\beta$ fibrillogenesis is limited to the processes occurring in the presence of (or triggered by) lipid, perhaps due to the alteration of bilayers properties by ASLPs.

ASLPs Swell in the Presence of TBLE Bilayers. To elucidate how ASLPs inhibit $\text{A}\beta_{1-40}$ induced bilayer disruption, the interaction between bilayers and ASLPs was explored. It is important to note previous studies that demonstrated inhibition of $\text{A}\beta_{1-40}$ TBLE bilayer disruption by lowering the cholesterol content of the bilayer by treatment with methyl- β -cyclodextrin²⁴ and that the addition of cholesterol to sphingomyelin bilayers increased $\text{A}\beta_{1-40}$ binding and aggregation.⁴⁷ It has also been shown that $\text{A}\beta$ can insert into cholesterol-containing phosphatidylcholine monolayers and displace the sterol.⁴⁸ As lipoproteins play a role in extracellular cholesterol transport, these observations point to the possibility that the apoE-containing ASLPs could modulate the cholesterol content of the TBLE bilayers. To test this hypothesis, apoE3-containing ASLPs were exposed to supported TBLE bilayers, collected, and imaged *in situ* on mica. ASLP size distributions were determined by quantitative image analysis using tip contribution correction methods.⁴⁹ In previous studies carried out with nascent lipoprotein particles, apoE3-containing ASLPs appeared as flat discoidal nano-objects.⁴⁹ In comparison to these nascent apoE3-containing ASLPs, ASLPs exposed to bilayers increased in both volume and height, but not diameter (Figure 7). Their dimensions now closely resembled those observed for plasma HDLs.⁴⁹ The observed increase in volume is consistent with lipoprotein particles acquiring some component (most likely cholesterol and phospholipids) from bilayers. It is known that lipoprotein particles can acquire cholesterol and phospholipids from bilayers via aqueous diffusion and/or collisions.^{50–53} Cholesterol is relatively easily removed and inserted into lipid membranes, as modulation of

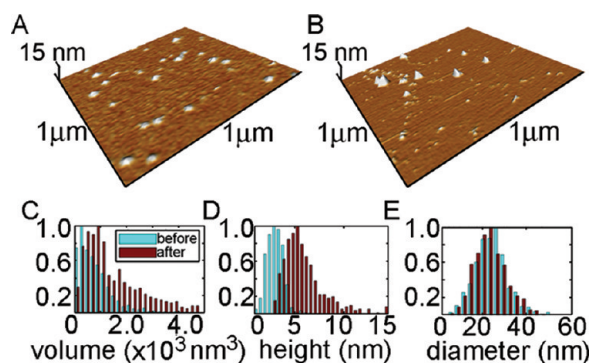


Figure 7. Comparison of apoE3-containing ASLPs before and after exposure to TBLE bilayers. 3D *in situ* AFM images of apoE3-containing ASLPs acquired before (A) and after (B) exposure to bilayers demonstrating swelling of ASLPs after exposure to the bilayers. Volume (C), height (D), and diameter (E) distributions for apoE3-containing ASLPs before and after exposure to supported lipid bilayers based on quantitative analysis of AFM images. The distributions of apoE3-containing ASLPs before exposure to TBLE were compiled from 20 images that were $3 \times 3 \mu\text{m}^2$ for a total number of 1120 particles measured. The distributions of apoE3-containing ASLPs after exposure to TBLE were compiled from 15 images that were $3 \times 3 \mu\text{m}^2$ for a total number of 563 particles measured.

cholesterol content is one way in which the fluidity of membranes is regulated in cells. Therefore, depletion of cholesterol content in bilayers, or the interaction of apoE-containing lipoproteins with cholesterol, could be one factor in inhibiting their disruption by $\text{A}\beta$. ASLPs could also be removing oxidatively damaged lipid components that have been shown to increase $\text{A}\beta$ aggregation,^{54–56} as apoE has been shown to have antioxidant activity.^{43,57–61}

ApoE3 and ApoE4 Appear to Alter Membrane Rigidity. Experiments described thus far indicate that rather than directly affecting $\text{A}\beta$ fibrillogenesis, ASLPs modulate $\text{A}\beta$'s interaction with lipid bilayers. As ASLPs apparently uptake bilayer components, suppression of $\text{A}\beta$ induced disruption of bilayers may be related to lipoproteins modulating bilayer properties. Depletion of cholesterol content and/or the removal of oxidatively damaged membrane components are two of the plausible scenarios. Cholesterol residing in bilayer membranes can alter acyl chain mobility, and the net effect of cholesterol on bilayer fluidity varies based on lipid composition and temperature.^{62–65} At the lipid content and concentrations commonly found in eukaryotic plasma membranes, cholesterol usually results in increased membrane rigidity.^{62–65} Oxidative modifications of polyunsaturated fatty acids generally increase the rigidity of lipid bilayer membranes due to steric hindrance restricting the movement of lipid acyl chains.^{66,67} Peroxidation of lipid components of membranes is a possible explanation for age-dependent reduction of membrane fluidity.^{67,68} Given the indication that ASLPs sequester away bilayer components, changes in the mechanical properties of the bilayers can be expected. TBLE bilayers contain a large percentage of cholesterol and are susceptible to oxidative damage. Removal of cholesterol and peroxidized lipid components from the bilayer would alter its fluidity by making the membrane softer, potentially making the bilayers less susceptible to $\text{A}\beta_{1-40}$ disruption. This is supported by observations that $\text{A}\beta$ preferentially accumulates on gel phase domains of lipid bilayers as opposed to fluid domains.⁶⁹ It has also been observed that $\text{A}\beta$

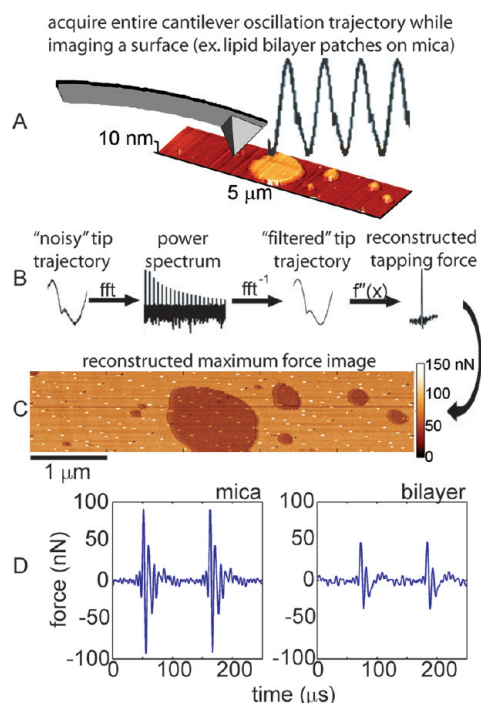


Figure 8. Scanning probe acceleration microscopy allows for the indirect measurement of mechanical properties by reconstructing the instantaneous tip/sample force in tapping mode AFM. Exposed mica is clearly seen in a standard (A) height image of bilayer patches. (B) The trajectory of the cantilever is filtered using Fourier transform, and the second derivative of the cantilever trajectory is used to reconstruct the tip/sample tapping force. (C) A reconstructed map of the maximum tapping forces demonstrates that imaging forces can be used to construct spatially resolved maps of surface properties. The diagonal white dots in the image are an artifact due to acquiring the deflection signal with a fixed sampling rate. (D) Reconstructed tip/sample force interactions in regions corresponding to mica and bilayer.

preferentially accumulates on oxidatively damaged lipids compared to nonoxidatively damaged lipids.⁵⁴

To establish if exposure to apoE-containing ASLPs altered bilayer fluidity, SPAM⁴⁴ analysis of bilayer rigidity was performed. The suitability of this technique for this purpose stems from its ability to partially reconstruct time-resolved forces acting between the AFM tip and sample surface in a tapping mode experiment based on the analysis of the cantilever deflection signal (Figure 8). Although the average force per oscillation cycle remains constant at any given set of operation parameters, specific features of time-resolved tip/sample force interactions change in response to different mechanical properties of surfaces. For example, the contact time increases for softer samples while the maximum tapping force (F_{\max}) is reduced. Due to the direct correlation between maximum tapping force and surface rigidity, maximum tapping force maps provide information about the relative rigidity of surfaces. When comparing topography (Figure 8A) and F_{\max} (Figure 8C) images of supported lipid bilayer patches on mica, it is apparent that contrast in the F_{\max} image can distinguish between bilayers (darker patches in Figure 8C) and mica (brighter areas in Figure 8C).

Force maps were constructed for bilayer patches on mica before and 2 h after treatment with either apoE3- or apoE4-containing ASLPs (Figure 9). Histograms of F_{\max} reveal that F_{\max} associated with the bilayer decreased after the addition of the

lipoproteins (Figure 9I,J), representing a softening or increase in fluidity of the bilayer (F_{\max} associated with mica acts as an internal control). As removal of cholesterol and peroxidated lipids is a known mechanism to alter bilayer stiffness, this supports the notion that ASLPs extract these types of components from bilayers. Comparisons between experiments are complicated by the fact that a new cantilever is needed for each run to prevent contamination, resulting in slightly different values of F_{\max} in each experiment (compare the scales for Figure 9I,J). Despite this complication, comparisons of the relative shift of maximum tapping force associated with the bilayer can be made.⁷⁰ In this regard, it appears that apoE3-containing ASLPs soften the bilayer to a greater extent than their apoE4-containing counterparts, as the relative shift in maximum tapping force is much greater. This observation might be one of the factors making apoE3 more effective in protecting TBLE bilayers from $A\beta$ -induced disruption.

While the ability of $A\beta_{1-40}$ to disrupt supported TBLE bilayers has already been described elsewhere,^{23,24} studies described here illustrate that apoE3- and apoE4-containing ASLPs are capable of inhibiting $A\beta_{1-40}$ induced bilayer disruption, with apoE3 being more efficient in this regard. The protective action of ASLPs may be due to their ability to alter the TBLE bilayers (e.g., through cholesterol and/or oxidatively damaged lipid extraction), as demonstrated by particle size and SPAM analysis. As lipoproteins are known to function in cholesterol transport, this is one plausible scenario, and senile plaques composed of $A\beta$ have been shown to be enriched in cholesterol content in AD patient brains.⁷¹ Furthermore, the ability of $A\beta$ to be incorporated into cellular membranes was shown to be dependent on cholesterol, with high cholesterol content in membranes being associated with increased $A\beta$ incorporation and cell death.⁷² However, apoE has also been shown to have antioxidant activity in cell culture and *in vivo*,^{58–61} and the protective properties of apoE-containing ASLPs could be due to their ability to act as antioxidants. This could also explain the isoform dependence observed here, as it has been shown that conditioned medium from apoE-transfected macrophage cell culture protects neuronal cell culture against oxidative environments in an isoform dependent manner.⁴³ These observations suggest that the role of different apoE isoforms in AD may, after all, lie in their respective ability to efficiently sequester and transport membrane components, such as cholesterol or oxidatively damaged lipids, in the CNS.

As the major risk factor associated with AD is aging, changes in membrane composition and physical properties associated with aging may play a role in increasing cellular susceptibility to $A\beta$ cytotoxicity. Both enhanced cellular cholesterol content^{71,73,74} and oxidative damage^{67,75} are associated with aging, decreased fluidity of membranes, and AD. The continuous production of reactive oxygen species (ROS) has been one of the major focuses of age related research since the “free radical theory” of aging was first proposed.^{76–78} This theory simply states that aging results in damage generated by the production of ROS.⁷⁹ The potential importance of ROS generation in aging is underscored by the existence of enzymes that function to prevent or counteract the damage caused by such species.⁸⁰ Oxidative modifications of polyunsaturated fatty acids generally increase the rigidity of lipid bilayer membranes due to steric hindrance restricting the movement of lipid acyl chains.^{66,67} Importantly, $A\beta$ oligomers preferentially accumulate near the plasma membrane of oxidatively damaged cells⁸¹ and evidence of enhanced oxidative damage is

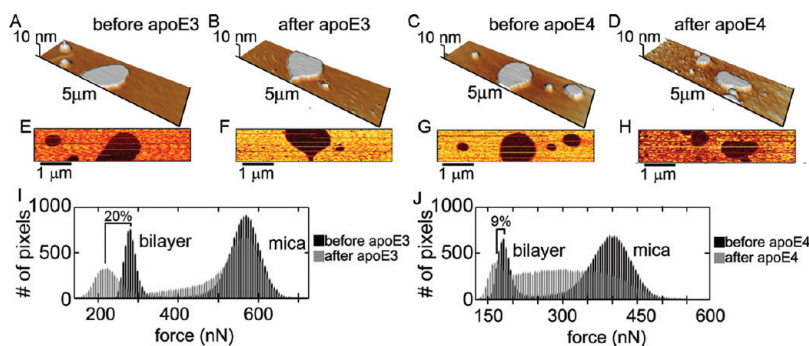


Figure 9. SPAM analysis demonstrating the impact of apoE3- and apoE4-containing ASLPs on TBLE bilayer rigidity. To facilitate comparison, TBLE samples were prepared as isolated bilayer patches on mica (A–D), providing an internal reference as shown in height images. The values of F_{\max} are directly related to the rigidity of the surface, with softer surfaces resulting in smaller values of F_{\max} . In all F_{\max} maps (E–H), bilayers appeared as darker (softer) regions. (I, J) Histograms of F_{\max} were distinctly bimodal, with modes corresponding to the mica and bilayer surfaces. After the addition of apoE-containing ASLPs, the mode corresponding to the bilayer shifted, indicating bilayer softening. This shift was less pronounced for apoE4-containing ASLPs (~9% compared to ~20% for apoE3), indicating that they were less effective in altering the rigidity of bilayers.

observed in AD brains.^{82,83} The ability of apoE-containing lipoprotein particles to influence membrane composition by removing cholesterol or oxidatively damaged membrane components may play an important role in counteracting these age-related changes.

There is mounting evidence that the cytotoxic effects of $A\beta$ may be associated with its interaction with cellular membranes. Several studies have reported that $A\beta$ directly binds to membrane components leading to physical changes in membrane properties.^{84–86} While it is well documented that surfaces can influence aggregate morphology and stability,^{87–91} the composition and biophysical properties of membranes appear to also have an impact on $A\beta$ conformation, insertion into the membrane, and aggregation.^{24,72,92} Electrostatic interactions with surfaces can also have a pronounced effect on $A\beta$ aggregation. It has been demonstrated that aggregation of $A\beta$ on a negatively charged mica surface is markedly different compared to aggregation on a neutral graphite surface.⁹⁰ Even without changing the surface charge, altering the charge of the $A\beta$ peptide by introduction of disease-related point mutations can lead to unique aggregation on both mica⁹¹ and TBLE bilayer surfaces.⁹³ Changes in bilayer composition observed here could also potentially change the surface charge of the membrane, potentially influencing the ability of $A\beta$ to aggregate and disrupt the bilayer. For example, removal of neutral cholesterol molecules could potentially increase the charge density by allowing the charged head groups of other lipid components to pack more efficiently. It has also often been observed that exogenously added $A\beta$ will selectively bind a subset of cells in an apparent homogeneous population of cells in culture.^{94–96} This selectivity may also be influenced by specific lipid interactions,^{97–100} which would be directly related to membrane composition. ApoE-containing ASLPs were able to directly influence the biophysical properties of the model lipid membranes used in this study by uptake of membrane components with the efficiency of this process being isoform dependent. This ability of lipoprotein particles may play a role in modifying the ability of $A\beta$ to bind to cells by controlling membrane composition. While precise mechanisms by which $A\beta$ aggregates are toxic remain unclear, $A\beta$ binding to cellular and subcellular membranes represents a potentially fundamental step in AD pathology.

Although the studies presented here do not provide any direct evidence of the interaction of $A\beta_{1–40}$ with ASLPs, the possibility

that apoE3 and apoE4 ASLPs altered the $A\beta_{1–40}$ aggregation pathway itself cannot be completely ruled out. Previous studies demonstrated that lipid-free apoE bound to $A\beta$ to form stable complexes and that apoE4 bound $A\beta$ more rapidly.^{101,102} Later studies with lipidated forms of apoE found that apoE3 (and apoE2) would form complexes with $A\beta$ more efficiently than apoE4.^{103–105} However, it is apparent that apoE does have an effect on $A\beta$ in the presence of lipids and/or cholesterol, pointing to the importance of incorporating all of these factors in designing experiments aimed at elucidating the interaction between apoE and $A\beta$. The observation that fresh solutions of $A\beta_{1–40}$ were required to induce bilayer disruption is consistent with the notion that early, prefibrillar forms of $A\beta_{1–40}$ might play a key role in toxicity. This notion, which is supported by several different studies,^{106–109} continues to receive considerable attention in the field of AD. Potential candidates for such toxic species include soluble $A\beta$ oligomers or amyloid-derived diffusible ligands (ADDLs)¹¹⁰ and $A\beta^*56$ oligomers.¹¹¹

The suppression of $A\beta$ conversion to a fibrillar form by apoE3 and apoE4 in the presence of TBLE bilayers is consistent with observations from a mouse model of AD demonstrating that human apoE3 and E4 suppress $A\beta$ deposition in vivo. GFAP-apoE2, -apoE3, and -apoE4[±] transgenic mice expressing similar levels of human apoE by astrocytes in the absence of mouse apoE to PDAPP^{+/+}, apoE^{-/-} mice were bred, and analysis of these mice revealed several interesting findings.^{38,112,113} $A\beta$ deposits began to develop by 9 months of age in PDAPP[±] mice in the presence or absence of mouse apoE, and these deposits increased dramatically by 15 months of age ($\text{apoE}^{+/+} \gg \text{apoE}^{-/-}$ in absolute level; $\text{apoE}^{-/-}$ with no fibrillar $A\beta$). In contrast to the effects of mouse apoE or no apoE on $A\beta$ deposition, human apoE2, apoE3, and apoE4, expressed at comparable levels to endogenous mouse apoE, delayed $A\beta$ deposition until 15–24 months of age. At 15 months of age, some mice expressing apoE3 and apoE4 began to develop similar patterns of $A\beta$ deposition in the form of both diffuse and neuritic plaques as was observed in the presence of mouse apoE. Furthermore, $A\beta$ deposition and neuritic plaques were more abundant in apoE4 than apoE3 expressing mice. By 18–22 months of age, some apoE2-expressing mice had begun to develop diffuse plaques, but no neuritic plaques had developed. The different effects of human apoE on $A\beta$ as compared to murine apoE may be due to mouse apoE being only ~70% identical to human apoE at the amino acid

level, and it has been shown to have inherent functional differences compared with human apoE isoforms on plasma lipoprotein metabolism *in vivo*.¹¹⁴ Such data suggests a critical and isoform specific role for apoE in conversion of A β to a fibrillar form with ensuing neuritic plaque formation (E4 > E3 > E2). They also suggest that human apoE may play a role in A β clearance in addition to A β fibrillogenesis. The extent of lipidation of apoE also exerts influence on the levels of A β in the brains of transgenic mice.¹¹⁵ Our study here demonstrates that this effect on A β deposition may in part be due to the ability of apoE-containing ASLPs to regulate physical properties of bilayers.

With the use of more physiologically relevant substrates such as cells and lipid bilayers, obtaining physical insights into the formation of toxic aggregates and their modes of operation using AFM is becoming more feasible. The ability to directly image and measure changes in mechanical properties associated with specific interactions on increasingly physiologically relevant substrates in a "quasi" real-time fashion can provide new insights that are exceedingly difficult to obtain using other traditional methods. In the case of A β , its interaction with total brain lipid extract bilayers as observed by AFM^{24,93,116} is particularly useful as a model system since the observed disruption may represent one of A β 's potential toxic pathways. Such A β induced membrane disruption can be thus used to study the effect of relevant biomacromolecules and complexes on this process as was shown here for apoE-containing ASLPs. This provides the opportunity to explore the ability of potential therapeutic agents designed to inhibit A β aggregation and protect membranes from A β induced disruption. Similar studies developing model bilayer systems have been carried out with other conformational disease related proteins,¹¹⁷ indicating that these types of studies are feasible.

METHODS

Sample Preparation. Synthetic A β_{1-40} was obtained from AnaSpec Inc. (San Jose, CA) and dissolved in dimethyl sulfoxide (DMSO) to make two separate stock solutions at a concentration of 2.4 mg/mL. These stock solutions were then dissolved in phosphate-buffered saline (PBS) buffer (pH 7.3) to a final concentration of 48 μ g/mL (final DMSO concentration less than 2%). Astrocyte secreted apoE3- and apoE4-containing particles were prepared and purified as described earlier¹¹⁸ from transgenic mice expressing human apoE3 or apoE4.¹¹⁹ The isolation of astrocyte secreted lipoprotein particles, obtained from astrocyte culture media, was performed by antibody affinity chromatography. Total brain lipid extract (porcine) was purchased from Avanti Polar Lipids (Alabaster, AL), dried under a nitrogen stream, lyophilized, and resuspended in PBS (pH 7.3) at a concentration of 1 mg/mL. Using an acetone/dry ice bath, bilayers and multilayer lipid sheets were formed by five cycles of freeze–thaw treatment.^{23,24} The lipid suspensions were then sonicated for 15 min to promote vesicle formation. All experiments were performed with the same lot of lipids.

AFM Imaging Conditions. *In situ* AFM experiments were performed with a Nanoscope III MultiMode scanning probe microscope (Digital Instruments, Santa Barbara, CA) equipped with fluid cell and a vertical engage J-scanner. Images were taken with V-shaped oxide-sharpened silicon nitride cantilever with a nominal spring constant of 0.5 N/m. Scan rates were set at 1–2 Hz with cantilever drive frequencies ranging from ~8 to 10 kHz. Concentrated TBLE vesicle solution was added to the cell in 40 μ L aliquots by the hanging drop method and allowed to

fuse *in situ* on a freshly cleaved mica substrate. Once a 50 \times 50 μ m² patch of predominately defect-free bilayer was formed, the cell was flushed to remove vesicles remaining in solution. Only predominately defect-free bilayers that were 50 \times 50 μ m² were used for studies with A β . Then, a 30 μ L aliquot of PBS buffer (for control experiments) or ASLPs at an appropriate concentration was added to the fluid cell. After ~2 h, 20 μ L of 48 μ g/mL A β_{1-40} solution was added through the channels in the fluid cell, resulting in a final A β concentration of 9.6 μ g/mL. To study the possible interaction of ASLPs with the bilayers, the solution in the cell containing ASLPs was extracted after 2 h in some experiments via the fluid cell channels without the addition of any A β . These extracted ASLPs were imaged, and their sizes were analyzed using tip correction procedures and size analysis.⁴⁹

For experiments aimed at elucidating the aggregation of A β_{1-40} peptides under free solution conditions, 48 μ g/mL stock solutions of A β_{1-40} were allowed to aggregate at room temperature in microcentrifuge tubes. These solutions were sampled at 24 h intervals for five consecutive days by taking 5 μ L aliquots of each solution and spotting them on freshly cleaved mica. These depositions were washed with 200 μ L of HPLC grade water and dried under a gentle stream of nitrogen. A β aggregates deposited on mica were imaged *ex situ* using a Nanoscope III MultiMode scanning probe microscope (Veeco, Santa Barbara, CA) equipped with vertical engage J-scanner and operated in the tapping mode. Images were taken with a diving board shaped silicon cantilever with a nominal spring constant of 40 N/m. Scan rates were set at 2–3 Hz with cantilever drive frequencies of approximately 300 kHz.

For SPAM experiments designed to explore the effect of apoE-containing ASLPs on supported bilayers, 5 \times 1.25 μ m² images were captured at 256 \times 64 pixel resolution with other operation parameters set as described earlier. Cantilever deflection trajectories were simultaneously captured via a Nanoscope signal access module using a CompuScope 14100 data acquisition card (Gage, Lachine, Quebec) and custom written software. Trajectories were captured at 5–10 MS/s and 14 bit resolution. To ensure that areas of exposed mica would be present for an internal reference for SPAM experiments, 40 μ L of the suspended vesicle solution diluted 5 times was added directly to the cell using the hanging drop method, and placed on freshly cleaved mica, allowing the vesicles to flatten into bilayer patches. Once stable patches appeared, 20 μ L of 30 μ g/mL ASLP solution was added via the channels in the fluid cell and allowed to sit for 2 h before performing another SPAM experiment on the bilayer.

Quantitative Analysis of AFM Images. The AFM images gathered in this study were evaluated using software that automated size analysis of objects. The software locates individual objects in an AFM image and measures their volumes and heights and other geometrical characteristics and facilitates quick analysis of thousands of individual objects, organizing individual measurements into large data sets of which statistical measures could be made.^{49,120} Contributions due to the finite shape and size of the tip were compensated for, based on geometrical simulations as described previously.⁴⁹

AUTHOR INFORMATION

Corresponding Author

*(J.L.) E-mail: justin.legleiter@mail.wvu.edu. Telephone: (304) 293-3435 ext. 6436. Fax: (304) 293-4904. (T.K.) E-mail: tomek@andrew.cmu.edu. Telephone: (412) 268-5927. Fax: (412) 268-1061.

Author Contributions

Lipoprotein particle purification was performed by J.D.F and D.M.H. Experiment design, peptide preparation, and AFM characterizations were accomplished by J.L. and T.K. Data analysis, writing, and editing were completed by J.L., D.M.H., and T.K.

Funding Sources

The authors would like to acknowledge NSF Grants NSF-CTS-0304568 and NSF-DMR-9974457 and NIH Grant R37 AG13956.

■ ABBREVIATIONS

AD, Alzheimer's disease; $A\beta$, amyloid- β peptide; apoE, apolipoprotein E; ASLPS, astrocyte secreted lipoprotein particles; AFM, atomic force microscopy; APP, β -amyloid precursor protein; CNS, central nervous system; PBS, phosphate-buffered saline; rms, root-mean-square; SPAM, scanning probe acceleration microscopy; TBLE, total brain lipid extract

■ REFERENCES

- (1) Selkoe, D. J. (2001) Alzheimer's Disease: Genes, Proteins, and Therapy. *Physiol. Rev.* 81, 741–766.
- (2) Hardy, J., and Selkoe, D. J. (2002) The amyloid hypothesis of Alzheimer's disease: Progress and problems on the road to therapeutics. *Science* 297, 353–356.
- (3) Lansbury, P. T., Jr. (1996) A reductionist view of Alzheimer's disease. *Acc. Chem. Res.* 29, 317–321.
- (4) Kelly, J. W. (1998) The alternative conformations of amyloidogenic proteins and their multi-step assembly pathways. *Curr. Opin. Struct. Biol.* 8, 101–106.
- (5) Smith, M. A. (1998) Alzheimer disease. *Int. Rev. Neurobiol.* 42, 1–54.
- (6) Nitsch, R. M., Blusztajn, J. K., Pittas, A. G., Slack, B. E., Growdon, J. H., and Wurtman, R. J. (1992) Evidence for a membrane defect in Alzheimer disease brain. *Proc. Natl. Acad. Sci. U.S.A.* 89, 1671–1675.
- (7) Soderberg, M., Edlund, C., Alafuzoff, I., Kristensson, K., and Dallner, G. (1992) Lipid composition in different regions of the brain in Alzheimer's disease/senile dementia of Alzheimer's type. *J. Neurochem.* 59, 1646–1653.
- (8) Svennerholm, L., and Gottfries, C.-G. (1994) Membrane lipids, selectively diminished in Alzheimer brains, suggest synapse loss as a primary event in early-onset form (type I) and demy-elination in late-onset form (type II). *J. Neurochem.* 62, 1039–1047.
- (9) Weigiel, J., and Wisniewski, H. M. (1990) The complex of microglial cells and amyloid star in three-dimensional reconstruction. *Acta Neuropathol.* 81, 116–124.
- (10) Yamaguchi, H., Nakazato, Y., Hirai, S., Shoji, M., and Harigaya, Y. (1989) Electron micrograph of diffuse plaques. Initial stage of senile plaque formation in the Alzheimer brain. *Am. J. Pathol.* 135, 593–597.
- (11) Arispe, N., Rojas, E., and Pollard, H. B. (1993) Alzheimer-Disease Amyloid Beta-Protein Forms Calcium Channels in Bilayer-Membranes - Blockade by Tromethamine and Aluminum. *Proc. Natl. Acad. Sci. U.S.A.* 90, 567–571.
- (12) Choo-Smith, L.-P., and Surewicz, W. K. (1997) Acceleration of amyloid fibril formation by specific binding of $Ab(1–40)$ peptide to ganglioside-containing membrane vesicles. *FEBS Lett.* 402, 95–98.
- (13) Mason, R. P., Estermeyer, J. D., Kelly, J. F., and Mason, P. E. (1996) Alzheimer's disease amyloid- β peptide 25–35 is localized in the membrane hydrocarbon core: x-ray diffraction analysis. *Biochem. Biophys. Res. Commun.* 222, 78–82.
- (14) McLaurin, J., and Chakrabarty, A. (1997) Characterization of the interactions of Alzheimer b-amyloid peptides with phospholipid membranes. *Eur. J. Biochem.* 245, 355–363.
- (15) McLaurin, J., Yang, D.-S., Yip, C. M., and Fraser, P. E. (2000) Modulating factors in amyloid- β fibril formation. *J. Struct. Biol.* 130, 259–270.
- (16) Mirzabekov, T., Lin, M.-C., Yuan, W.-L., Marshall, D. J., Carman, M., Tomaselli, K., Leiberburg, I., and Kagan, B. L. (1994) Channel formation in planar lipid bilayers by a neurotoxic fragment of the b -amyloid peptide. *Biochem. Biophys. Res. Commun.* 202, 1142–1148.
- (17) Pillot, T., Drouet, B., Queille, S., Labeyre, C., Vandekerckhove, J., Rosseneu, M., Pincon-Raymond, M., and Chambaz, J. (1999) The nonfibrillar amyloid β -peptide induces apoptotic neuronal cell death: involvement of its C-terminal fusogenic domain. *J. Neurochem.* 73, 1626–1634.
- (18) Terzi, E., Holzemann, G., and Seelig, J. (1994) Alzheimer β -amyloid peptide 25–35: electrostatic interactions with phospholipid membranes. *Biochemistry* 33, 7434–7441.
- (19) Terzi, E., Holzemann, G., and Seelig, J. (1995) Self-association of β -amyloid peptide (1–40) in solution and binding to lipid membranes. *J. Mol. Biol.* 252, 633–642.
- (20) Gorbenko, G. P., and Kinnunen, P. K. J. (2006) The role of lipid-protein interactions in amyloid-type protein fibril formation. *Chem. Phys. Lipids* 141, 72–82.
- (21) Morita, M., Vestergaard, M., Hamada, T., and Takagi, M. (2010) Real-time observation of model membrane dynamics induced by Alzheimer's amyloid beta. *Biophys. Chem.* 147, 81–86.
- (22) Wong, P. T., Schauerte, J. A., Wisser, K. C., Ding, H., Lee, E. L., Steel, D. G., and Gafni, A. (2009) Amyloid-beta Membrane Binding and Permeabilization are Distinct Processes Influenced Separately by Membrane Charge and Fluidity. *J. Mol. Biol.* 386, 81–96.
- (23) Yip, C. M., and McLaurin, J. (2001) Amyloid- β Assembly: A Critical Step in Fibrillogenesis and Membrane Disruption. *Biophys. J.* 80, 1359–1371.
- (24) Yip, C. M., Elton, E. A., Darabie, A. A., Morrison, M. R., and McLaurin, J. (2001) Cholesterol, a Modulator of Membrane-associated $A\beta$ -Fibrillogenesis and Neurotoxicity. *J. Mol. Biol.* 311, 723–734.
- (25) Mahley, R. W. (1988) Apolipoprotein E: cholesterol transport protein with expanding role in cell biology. *Science* 240, 622–630.
- (26) Herz, J., and Willnow, T. E. (1995) Lipoprotein and receptor interactions in vivo. *Curr. Opin. Lipidol.* 6, 97–103.
- (27) Das, H. K., McPherson, J., Bruns, G. A., Karathanasis, S. K., and Breslow, J. L. (1985) Isolation, characterization, and mapping to chromosome 19 of the human apolipoprotein E gene. *J. Biol. Chem.* 260, 6240–6247.
- (28) Mauch, D. H., Nagler, K., Schumacher, S., Goritz, C., Muller, E.-C., Otto, A., and Pfrieger, F. W. (2001) CNS Synaptogenesis Promoted by Glia-Derived Cholesterol. *Science* 294, 1354–1357.
- (29) Pitas, R. E., Boyles, J. K., Lee, S. H., Foss, D., and Mahley, R. W. (1987) Astrocytes synthesize apolipoprotein E and metabolize apolipoprotein E-containing lipoproteins. *Biochim. Biophys. Acta* 917, 148–161.
- (30) Boyles, J. K., Pitas, R. E., Wilson, E., Mahley, R. W., and Taylor, J. M. (1985) Apolipoprotein E associated with astrocytic glia of the central nervous system and with nonmyelinating glia of the peripheral nervous system. *J. Clin. Invest.* 76, 1501–1513.
- (31) Basu, S. K., Ho, Y. K., Brown, M. S., Bilheimer, D. W., Anderson, R. G., and Goldstein, J. L. (1982) Biochemical and genetic studies of the apoprotein E secreted by mouse macrophages and human monocytes. *J. Biol. Chem.* 257, 9788–9795.
- (32) Stone, D. J., Rozovsky, I., Morgan, T. E., Anderson, C. P., Hajian, H., and Finch, C. E. (1997) Astrocytes and microglia respond to estrogen with increased apoE mRNA in vivo and in vitro. *Exp. Neurol.* 143, 313–318.
- (33) Pitas, R., Boyles, J., Lee, S., Hui, D., and Weisgraber, K. (1987) Lipoproteins and their receptors in the central nervous system. Characterization of the lipoproteins in cerebrospinal fluid and identification of apolipoprotein B, E (LDL) receptors in the brain. *J. Biol. Chem.* 262, 5380–5389.
- (34) Corder, E. H., Saunders, A. M., Strittmatter, W. J., Schmeichel, D. E., Gaskell, P. C., Small, G. W., Roses, A. D., Haines, J. L., and Pericak-Vance, M. A. (1993) Gene dose of apolipoprotein E type 4 allele and the risk of Alzheimer's disease in late onset families. *Science* 261, 921–923.
- (35) Mayeux, R., Stern, Y., Ottman, R., Tatemichi, T. K., Tang, M. X., Maestre, G., Ngai, C., Tycko, B., and Ginsberg, H. (1993) The

- apolipoprotein epsilon 4 allele in patients with Alzheimer's disease. *Ann. Neurol.* 34, 752–754.
- (36) Poirier, J., Davignon, J., Bouthillier, D., Kogan, S., Bertrand, P., and Gauthier, S. (1993) Apolipoprotein E polymorphism and Alzheimer's disease. *Lancet* 342, 697–699.
- (37) Buttini, M., Yu, G.-Q., Shockley, K., Huang, Y., Jones, B., Masliah, E., Mallory, M., Yeo, T., Longo, F. M., and Mucke, L. (2002) Modulation of Alzheimer-like synaptic and cholinergic deficits in transgenic mice by human apolipoprotein E depends on isoform, aging, and overexpression of amyloid peptides but not on plaque formation. *J. Neurosci.* 22, 10539–10548.
- (38) Holtzman, D. M., Bales, K. R., Tenkova, T., Fagan, A. M., Parsadanian, M., Sartorius, L. J., Mackey, B., Olney, J., McKeel, D., Wozniak, D., and Paul, S. M. (2000) Apolipoprotein E isoform-dependent amyloid deposition and neuritic degeneration in a mouse model of Alzheimer's disease. *Proc. Natl. Acad. Sci. U.S.A.* 97, 2892–2897.
- (39) Castano, E. M., Prelli, F., Wisniewski, T., Golabek, A., Kumar, R. A., Soto, C., and Frangione, B. (1995) Fibrillogenesis in Alzheimer's disease of amyloid beta peptides and apolipoprotein E. *Biochem. J.* 306, 599–604.
- (40) Ma, J., Yee, A., Brewer, B., Das, S., and Potter, H. (1994) Amyloid-associated proteins a-1-antichymotrypsin and apolipoprotein E promote assembly of Alzheimer b-protein into filaments. *Nature* 372, 92–94.
- (41) Bales, K. R., Verina, V., Cummins, D. J., Du, Y., Dodel, R. C., Saura, J., Fishman, C. E., DeLong, C. A., Piccardo, P., Petegnieff, V., Ghetti, B., and Paul, S. M. (1999) Apolipoprotein E is essential for amyloid deposition in the APP(V717F) transgenic mouse model of Alzheimer's disease. *Proc. Natl. Acad. Sci. U.S.A.* 96, 15233–15238.
- (42) DeMattos, R. B., Cirrito, J., Parsadanian, M., May, P. C., O'dell, M. A., Taylor, J. W., Harmony, J. A. K., Aronow, B. J., Bales, K. R., Paul, S. M., and Holtzman, D. M. (2004) ApoE and clusterin cooperatively suppress Ab levels and deposition. Evidence that apoE regulates extracellular Ab metabolism in vivo. *Neuron* 41, 193–202.
- (43) Miyata, M., and Smith, J. D. (1996) Apolipoprotein E allele-specific antioxidant activity and effects on cytotoxicity by oxidative insults and beta-amyloid peptides. *Nat. Genet.* 14, 55–61.
- (44) Legleiter, J., Park, M., Cusick, B., and Kowalewski, T. (2006) Scanning probe acceleration microscopy (SPAM) in fluids: mapping mechanical properties of surfaces at the nanoscale. *Proc. Natl. Acad. Sci. U.S.A.* 103, 4813–4818.
- (45) Jass, J., Tjärnhage, T., and Puu, G. (2000) From liposomes to supported, planar bilayer structures on hydrophilic and hydrophobic surfaces: an atomic force microscopy study. *Biophys. J.* 79, 3153–3163.
- (46) Legleiter, J., Czilli, D., Demattos, R., Gitter, B., Holtzman, D., and Kowalewski, T. (2004) Effect of different anti-Ab antibodies on Ab fibrillogenesis as assessed by atomic force microscopy. *J. Mol. Biol.* 335, 997–1006.
- (47) Devanathan, S., Salamon, Z., Lindblom, G., Gröbner, G., and Tollin, G. (2006) Effects of sphingomyelin, cholesterol and zinc ions on the binding, insertion and aggregation of the amyloid-b(1–40) peptide in solid-supported lipid bilayers. *FEBS J.* 273, 1389–1402.
- (48) Ashley, R. H., Harroun, T. A., Hauss, T., Breen, K. C., and Bradshaw, J. P. (2006) Autoinsertion of soluble oligomers of Alzheimer's Ab(1–42) peptide into cholesterol-containing membranes is accompanied by relocation of the sterol towards the bilayer surface. *BMC Struct. Biol.* 6, 21.
- (49) Legleiter, J., Demattos, R., Holtzman, D., and Kowalewski, T. (2004) In situ AFM studies of astrocyte-secreted apolipoprotein E and J-containing lipoproteins. *J. Colloid Interface Sci.* 278, 96–106.
- (50) Lange, Y., Molinaro, A. L., Chauncey, T. R., and Steck, T. L. (1983) On the mechanism of transfer of cholesterol between human erythrocytes and plasma. *J. Biol. Chem.* 258, 6920–6926.
- (51) Bottum, K., and Jonas, A. (1995) Cholesterol transfer from low density lipoproteins to reconstituted high density lipoproteins is determined by the properties and concentrations of both particles? *Biochemistry* 34, 7264–7270.
- (52) McLean, L. R., and Phillips, M. C. (1981) Mechanism of cholesterol and phosphatidylcholine exchange or transfer between unilamellar vesicles. *Biochemistry* 20, 2893–2900.
- (53) Liscum, L., and Underwood, K. W. (1995) Intracellular cholesterol transport and compartmentation. *J. Biol. Chem.* 270, 15443–15446.
- (54) Koppaka, V., and Axelsen, P. H. (2000) Accelerated Accumulation of Amyloid b; Proteins on Oxidatively Damaged Lipid Membranes. *Biochemistry* 39, 10011–10016.
- (55) Koppaka, V., Paul, C., Murray, I. V. J., and Axelsen, P. H. (2003) Early Synergy between Ab42 and Oxidatively Damaged Membranes in Promoting Amyloid Fibril Formation by Ab40*. *J. Biol. Chem.* 278, 36277–36284.
- (56) Murray, I. V. J., Liu, L., Komatsu, H., Uryu, K., Xiao, G., Lawson, J. A., and Axelsen, P. H. (2007) Membrane-mediated Amyloidogenesis and the Promotion of Oxidative Lipid Damage by Amyloid b Proteins. *J. Biol. Chem.* 282, 9335–9345.
- (57) Montine, K., Reich, E., Neely, M., Sidell, K., Olson, S., Markesberry, W., and Montine, T. (1998) Distribution of reducible 4-hydroxynonenal adduct immunoreactivity in Alzheimer disease is associated with APOE genotype. *J. Neuropathol. Exp. Neurol.* 57, 415–425.
- (58) Montine, K., Olson, S., Amarnath, V., Whetsell, J., WO, Graham, D., and Montine, T. (1997) Immunohistochemical detection of 4-hydroxy-2-nonenal adducts in Alzheimer's disease is associated with inheritance of APOE4. *Am. J. Pathol.* 150, 437–443.
- (59) Keller, J., Lauderback, C., Butterfield, D., Kindy, M., Yu, J., and Markesberry, W. (2000) Amyloid Ab-peptide effects on synaptosomes from apolipoprotein E-deficient mice. *J. Neurochem.* 74, 1579–1586.
- (60) Hayek, T., Oiknine, J., Brook, J. G., and Aviram, M. (1994) Increased Plasma and Lipoprotein Lipid Peroxidation in apo E-Deficient Mice. *Biochem. Biophys. Res. Commun.* 201, 1567–1574.
- (61) Matthews, R. T., and Flint Beal, M. (1996) Increased 3-nitrotyrosine in brains of Apo E-deficient mice. *Brain Res.* 718, 181–184.
- (62) Buffone, M. G., Verstraeten, S. V., Calamera, J. C., and Doncel, G. F. (2009) High Cholesterol Content and Decreased Membrane Fluidity in Human Spermatozoa Are Associated With Protein Tyrosine Phosphorylation and Functional Deficiencies. *J. Androl.* 30, 552–558.
- (63) Kojro, E., Gimpl, G., Lammich, S., Marz, W., and Fahrenholz, F. (2001) Low cholesterol stimulates the nonamyloidogenic pathway by its effect on the alpha-secretase ADAM 10. *Proc. Natl. Acad. Sci. U.S.A.* 98, 5815–5820.
- (64) Lemmich, J., Mortensen, K., Ipsen, J. H., Hønger, T., Bauer, R., and Mouritsen, O. G. (1997) The effect of cholesterol in small amounts on lipid-bilayer softness in the region of the main phase transition. *Eur. J. Biochem.* 25, 293–304.
- (65) Rappolt, M., Vidal, M. F., Kriechbaum, M., Steinhart, M., Amenitsch, H., Bernstorff, S., and Lagner, P. (2003) Structural, dynamic and mechanical properties of POPC at low cholesterol concentration studied in pressure/temperature space. *Eur. J. Biochem.* 31, 575–585.
- (66) Choi, J.-H., and Yu, B. P. (1995) Brain synaptosomal aging: Free radicals and membrane fluidity. *Free Radical Biol. Med.* 18, 133–139.
- (67) Choe, M., Jackson, C., and Yu, B. P. (1995) Lipid peroxidation contributes to age-related membrane rigidity. *Free Radical Biol. Med.* 18, 977–984.
- (68) Chen, J. J., and Yu, B. P. (1994) Alterations in mitochondrial membrane fluidity by lipid peroxidation products. *Free Radical Biol. Med.* 17, 411–418.
- (69) Choucair, A., Chakrapani, M., Chakravarthy, B., Katsaras, J., and Johnston, L. J. (2007) Preferential accumulation of Ab(1–42) on gel phase domains of lipid bilayers: An AFM and fluorescence study. *Biochim. Biophys. Acta, Biomembr.* 1768, 146–154.
- (70) Kumar, B., Pifer, P. M., Giovengo, A., and Legleiter, J. (2010) The effect of set point ratio and surface Young's modulus on maximum tapping forces in fluid tapping mode atomic force microscopy. *J. Appl. Phys.* 107, 044508.
- (71) Panchal, M., Loeper, J., Cossec, J.-C., Perruchini, C., Lazar, A., Pompon, D., and Duyckaerts, C. (2010) Enrichment of cholesterol in

- microdissected Alzheimer's disease senile plaques as assessed by mass spectrometry. *J. Lipid Res.* 51, 598–605.
- (72) Abramov, A. Y., Ionov, M., Pavlov, E., and Duchen, M. R. (2011) Membrane cholesterol content plays a key role in the neurotoxicity of β -amyloid: implications for Alzheimer's disease. *Aging Cell* 10, 595–603.
- (73) Cutler, R. G., Kelly, J., Storie, K., Pedersen, W. A., Tammara, A., Hatanpaa, K., Troncoso, J. C., and Mattson, M. P. (2004) Involvement of oxidative stress-induced abnormalities in ceramide and cholesterol metabolism in brain aging and Alzheimer's disease. *Proc. Natl. Acad. Sci. U.S.A.* 101, 2070–2075.
- (74) Wood, W. G., Schroeder, F., Igbaoboa, U., Avdulov, N. A., and Chochina, S. V. (2002) Brain membrane cholesterol domains, aging and amyloid beta-peptides. *Neurobiol. Aging* 23, 685–694.
- (75) Chen, C. S., Mrksich, M., Huang, S., Whitesides, G. M., and Ingber, D. E. (1997) Geometric Control of Cell Life and Death. *Science* 276, 1425–1428.
- (76) Harmon, D. (1956) Aging: a theory based on free radical and radiation chemistry. *J. Gerontol.* 11, 298–300.
- (77) Gerschman, R., Gilbert, D., Nye, S., Dwyer, P., and Fenn, W. (1954) Oxygen poisoning and x-irradiation: a mechanism in common. *Science* 119, 623–626.
- (78) Harman, D. (1981) The aging process. *Proc. Natl. Acad. Sci. U.S.A.* 78, 7124–7128.
- (79) Beckman, K., and Ames, B. (1998) The free radical theory of aging matures. *Physiol. Rev.* 78, 547–581.
- (80) de Magalhaes, J., and Church, G. (2006) Cells discover fire: employing reactive oxygen species in development and consequences for aging. *Exp. Gerontol.* 41, 1–10.
- (81) Cecchi, C., Fiorillo, C., Baglioni, S., Pensalfini, A., Bagnoli, S., Nacmias, B., Sorbi, S., Nosi, D., Relini, A., and Liguri, G. (2007) Increased susceptibility to amyloid toxicity in familial Alzheimer's fibroblasts. *Neurobiol. Aging* 28, 863–876.
- (82) Ansari, M. A., and Scheff, S. W. (2010) Oxidative Stress in the Progression of Alzheimer Disease in the Frontal Cortex. *J. Neuropath. Exp. Neurol.* 69, 155–167.
- (83) Williamson, R., Usardi, A., Hanger, D. P., and Anderton, B. H. (2008) Membrane-bound β -amyloid oligomers are recruited into lipid rafts by a fyn-dependent mechanism. *FASEB J.* 22, 1552–1559.
- (84) Friedman, R., Pellarin, R., and Caflisch, A. (2009) Amyloid Aggregation on Lipid Bilayers and Its Impact on Membrane Permeability. *J. Mol. Biol.* 387, 407–415.
- (85) Sokolov, Y., Kozak, J. A., Kayed, R., Chanturiya, A., Glabe, C., and Hall, J. E. (2006) Soluble Amyloid Oligomers Increase Bilayer Conductance by Altering Dielectric Structure. *J. Gen. Physiol.* 128, 637–647.
- (86) Terzi, E., Hölzemann, G., and Seelig, J. (1997) Interaction of Alzheimer b-amyloid peptide (1–40) with lipid membranes. *Biochemistry* 36, 14845–14852.
- (87) Blackley, H. K., Patel, N., Davies, M. C., Roberts, C. J., Tendler, S. J., Wilkinson, M. J., and Williams, P. M. (1999) Morphological development of Ab(1–40) amyloid fibrils. *Exp. Neurol.* 158, 437–443.
- (88) Blackley, H. K. L., Sanders, G. H. W., Davies, M. C., Roberts, C. J., Tendler, S. J. B., and Wilkinson, M. J. (2000) *In-Situ* Atomic Force Microscopy Study of b-Amyloid Fibrillization. *J. Mol. Biol.* 298, 833–840.
- (89) Goldsbury, C., Kistler, J., Aeby, U., Arvinte, T., and Cooper, G. J. S. (1999) Watching Amyloid Fibrils Grow by Time-Lapse Atomic Force Microscopy. *J. Mol. Biol.* 285, 33–39.
- (90) Kowalewski, T., and Holtzman, D. M. (1999) In situ atomic force microscopy study of Alzheimer's b-amyloid peptide on different substrates: new insights into mechanism of beta-sheet formation. *Proc. Natl. Acad. Sci. U.S.A.* 96, 3688–3693.
- (91) Yates, E. A., Cucco, E. M., and Legleiter, J. (2011) Point mutations in $\text{A}\beta$ induce polymorphic aggregates at liquid/solid interfaces. *ACS Chem. Neurosci.* 2, 294–307.
- (92) Bokvist, M., Lindstrom, F., Watts, A., and Grobner, G. (2004) Two types of Alzheimer's b-amyloid (1–40) peptide membrane interactions: aggregation preventing transmembrane anchoring versus accelerated surface fibril formation. *J. Mol. Biol.* 335, 1039–1049.
- (93) Pifer, P. M., Yates, E. A., and Legleiter, J. (2011) Point Mutations in A beta Result in the Formation of Distinct Polymorphic Aggregates in the Presence of Lipid Bilayers. *PLoS One* 6 e16248.
- (94) De Felice, F. G., Wu, D., Lambert, M. P., Fernandez, S. J., Velasco, P. T., Lacor, P. N., Bigio, E. H., Jerecic, J., Acton, P. J., Shughrue, P. J., Chen-Dodson, E., Kinney, G. G., and Klein, W. L. (2008) Alzheimer's disease-type neuronal tau hyperphosphorylation induced by $\text{A}[\beta]$ oligomers. *Neurobiol. Aging* 29, 1334–1347.
- (95) Lacor, P. N., Buniel, M. C., Chang, L., Fernandez, S. J., Gong, Y., Viola, K. L., Lambert, M. P., Velasco, P. T., Bigio, E. H., Finch, C. E., Kraft, G. A., and Klein, W. L. (2004) Synaptic Targeting by Alzheimer's-Related Amyloid β Oligomers. *J. Neurosci.* 24, 10191–10200.
- (96) Simakova, O., and Arispe, N. J. (2007) The Cell-Selective Neurotoxicity of the Alzheimer's A Peptide Is Determined by Surface Phosphatidylserine and Cytosolic ATP Levels. Membrane Binding Is Required for A Toxicity. *J. Neurosci.* 27, 13719–13729.
- (97) Lin, M.-S., Chen, L.-Y., Wang, S. S. S., Chang, Y., and Chen, W.-Y. (2008) Examining the levels of ganglioside and cholesterol in cell membrane on attenuation the cytotoxicity of beta-amyloid peptide. *Colloids Surf. B* 65, 172–177.
- (98) Martins, I. C., Kuperstein, I., Wilkinson, H., Maes, E., Vanbrabant, M., Jonckheere, W., Van Gelder, P., Hartmann, D., D'Hooge, R., De Strooper, B., Schymkowitz, J., and Rousseau, F. (2008) Lipids revert inert A beta amyloid fibrils to neurotoxic protofibrils that affect learning in mice. *EMBO J.* 27, 224–233.
- (99) Okada, T., Wakabayashi, M., Ikeda, K., and Matsuzaki, K. (2007) Formation of Toxic Fibrils of Alzheimer's Amyloid b-Protein-(1–40) by Monosialoganglioside GM1, a Neuronal Membrane Component. *J. Mol. Biol.* 371, 481–489.
- (100) Wakabayashi, M., and Matsuzaki, K. (2007) Formation of Amyloids by Ab-(1–42) on NGF-differentiated PC12 Cells: Roles of Gangliosides and Cholesterol. *J. Mol. Biol.* 371, 924–933.
- (101) Sanan, D. A., Weisgraber, K. H., Russell, S. J., Mahley, R. W., Huang, D., Saunders, A., Schmechel, D., Wisniewski, T., Frangione, B., Roses, A. D., and Strittmatter, W. J. (1994) Apolipoprotein-E Associates with Beta-Amyloid Peptide of Alzheimer's-Disease to Form Novel Monofibrils - Isoform Apoe4 Associates More Efficiently Than Apoe3. *J. Clin. Invest.* 94, 860–869.
- (102) Strittmatter, W. J., Weisgraber, K. H., Huang, D. Y., Dong, L. M., Salvesen, G. S., Pericak-Vance, M., Schmechel, D., Saunders, A. M., Goldgaber, D., and Roses, A. D. (1993) Binding of human apolipoprotein E to synthetic amyloid beta peptide: isoform-specific effects and implications for late-onset Alzheimer disease. *Proc. Natl. Acad. Sci. U.S.A.* 90, 8098–8102.
- (103) Aleshkov, S., Abraham, C. R., and Zannis, V. I. (1997) Interaction of nascent ApoE2, ApoE3, and ApoE4 isoforms expressed in mammalian cells with amyloid peptide beta (1–40). Relevance to Alzheimer's disease. *Biochemistry* 36, 10571–10580.
- (104) LaDu, M. J., Falduto, M. T., Manelli, A. M., Reardon, C. A., Getz, G. S., and Frail, D. E. (1994) Isoform-specific binding of apolipoprotein E to b-amyloid. *J. Biol. Chem.* 269, 23403–23406.
- (105) Yang, D. S., Smith, J. D., Zhou, Z. M., Gandy, S. E., and Martins, R. N. (1997) Characterization of the binding of amyloid-beta peptide to cell culture-derived native apolipoprotein E2, E3, and E4 isoforms and to isoforms from human plasma. *J. Neurochem.* 68, 721–725.
- (106) Demuro, A., Mina, E., Kayed, R., Milton, S. C., Parker, I., and Glabe, C. G. (2005) Calcium dysregulation and membrane disruption as a ubiquitous neurotoxic mechanism of soluble amyloid oligomers. *J. Biol. Chem.* 280, 17294–17300.
- (107) Lambert, M. P., Viola, K. L., Chromy, B. A., Chang, L., Morgan, T. E., Yu, J., Venton, D. L., Kraft, G. A., Finch, C. E., and Klein, W. L. (2001) Vaccination with soluble Ab oligomers generates toxicity-neutralizing antibodies. *J. Neurochem.* 79, 595–605.
- (108) Schauerte, J. A., Wong, P. T., Wisser, K. C., Ding, H., Steel, D. G., and Gafni, A. (2010) Simultaneous Single-Molecule Fluorescence and Conductivity Studies Reveal Distinct Classes of $\text{A}\beta$ Species on Lipid Bilayers. *Biochemistry* 49, 3031–3039.

- (109) Valincius, G. H., Frank, Budvytyte, R., Vanderah, D. J., McGillivray, D. J., Sokolov, Y., Hall, J. E., and Losche, M. (2008) Soluble Amyloid b-Oligomers Affect Dielectric Membrane Properties by Bilayer Insertion and Domain Formation: Implications for Cell Toxicity. *Biophys. J.* 95, 4845–4861.
- (110) Stine, W. B., Jr., Dahlgren, K. N., Krafft, G. A., and LaDu, M. J. (2003) In vitro characterization of conditions for amyloid- β peptide oligomerization and fibrillogenesis. *J. Biol. Chem.* 278, 11612–11622.
- (111) Lesné, S., MT, K., Kotilinek, L., Kayed, R., Glabe, C. G., Yang, A., Gallagher, M., and Ashe, K. H. (2006) A specific amyloid- β protein assembly in the brain impairs memory. *Nature* 440, 352–357.
- (112) Holtzman, D. M., Bales, K. R., Wu, S., Bhat, P., Parsadanian, M., Fagan, A. M., Chang, L. K., Sun, Y., and Paul, S. M. (1999) Expression of human apolipoprotein E reduces amyloid- β deposition in a mouse model of Alzheimer's disease. *J. Clin. Invest.* 103, R15–R21.
- (113) Fagan, A. M., Watson, M., Parsadanian, M., Bales, K. R., Paul, S. M., and Holtzman, D. M. (2002) Human and murine apoE markedly influence Ab metabolism both prior and subsequent to plaque formation in a mouse model of Alzheimer's disease. *Neurobiol. Dis.* 9, 305–318.
- (114) Sullivan, P. M., Mezdour, H., Aratani, Y., Knouff, C., Najib, J., Reddick, R. L., Quarfordt, S. H., and Nobuyo, M. (1997) Targeted replacement of the mouse apolipoprotein E gene with the common human APOE3 allele enhances diet-induced hypercholesterolemia and atherosclerosis. *J. Biol. Chem.* 272, 17972–17980.
- (115) Wahrle, S. E., Jiang, H., Parsadanian, M., Kim, J., Li, A. M., Knoten, A., Jain, S., Hirsch-Reinshagen, V., Wellington, C. L., Bales, K. R., Paul, S. M., and Holtzman, D. M. (2008) Overexpression of ABCA1 reduces amyloid deposition in the PDAPP mouse model of Alzheimer disease. *J. Clin. Invest.* 118, 671–682.
- (116) Yip, C. M., Darabie, A. A., and McLaurin, J. (2002) Ab42-Peptide Assembly on Lipid Bilayers. *J. Mol. Biol.* 318, 97–107.
- (117) Jo, E., McLaurin, J., Yip, C. M., St. George-Hyslop, P., and Fraser, P. E. (2000) a-Synuclein Membrane Interactions and Lipid Specificity. *J. Biol. Chem.* 275, 34328–34334.
- (118) DeMattos, R. B., Brendza, R. P., Heuser, J. E., Kierson, M., Cirrito, J. R., Fryer, J., Sullivan, P. M., Fagan, A. M., Han, X., and Holtzman, D. M. (2001) Purification and characterization of astrocyte-secreted apolipoprotein E and J-containing lipoproteins from wild-type and human apoE transgenic mice. *Neurochem. Int.* 39, 415–425.
- (119) Fagan, A. M., Holtzman, D. M., Munson, G., Mathur, T., Schneider, D., Chang, L. K., Getz, G. S., Reardon, C. A., Lukens, J., Shah, J. A., and LaDu, M. J. (1999) Unique lipoproteins secreted by primary astrocytes from wild type, apoE ($-/-$) and human apoE transgenic mice. *J. Biol. Chem.* 274, 30001–30007.
- (120) Burke, K. A., Godbey, J., and Legleiter, J. (2011) Assessing mutant huntingtin fragment and polyglutamine aggregation by atomic force microscopy. *Methods* 53, 275–284.